Contents lists available at ScienceDirect

EBioMedicine

Research paper

ATXN7L3 positively regulates SMAD7 transcription in hepatocellular carcinoma with growth inhibitory function

Ning Sun[a], Xinping Zhong[c], Shengli Wang[a], Kai Zeng[a], Hongmiao Sun[a], Ge Sun[a], Renlong Zou[a], Wei Liu[a], Wensu Liu[a], Lin Lin[a], Huijuan Song[a], Chi Lv[a,d], Chunyu Wang[a,#,*], Yue Zhao[a,b,#,*]

[a] Department of Cell Biology, Key laboratory of Cell Biology, Ministry of Public Health, and Key laboratory of Medical Cell Biology, Ministry of Education, School of Life Sciences, China Medical University, Shenyang City, Liaoning Province 110122, China
[b] Department of Endocrinology and Metabolism, Institute of Endocrinology, The First Affiliated Hospital of China Medical University, Shenyang City, Liaoning Province 110001, China
[c] Department of General Surgery, the First Affiliated Hospital of China Medical University, Shenyang City, Liaoning Province, 110001, China
[d] Department of General Surgery, Shengjing Hospital of China Medical University, Shenyang City, Liaoning Province, 110004, China

ARTICLE INFO

ABSTRACT

Background: Hepatocellular carcinoma (HCC) is a leading cause of cancer death worldwide, with unmet need for the pharmacological therapy. The functions of ATXN7L3 in HCC progression are not known.
Methods: RNA sequence, quantitative real-time PCR, and western blot were performed to detect gene expression. Chromatin immunoprecipitation was performed to detect possible mechanisms. Immunohistochemical stain was performed to examine the protein expression. Colony formation, cell growth curve and xenograft tumor experiments were performed to examine cell growth in vitro and in vivo.
Findings: ATXN7L3 functions as a coactivator for ERα-mediated transactivation in HCC cells, thereby contributing to enhanced SMAD7 transcription. ATXN7L3 is recruited to the promoter regions of SMAD7 gene, thereby regulating histone H2B ubiquitination level, to enhance the transcription of SMAD7. A series of genes regulated by ATXN7L3 were identified. Moreover, ATXN7L3 participates in suppression of tumor growth. In addition, ATXN7L3 is lower expressed in HCC samples, and the lower expression of ATXN7L3 positively correlates with poor clinical outcome in patients with HCC.
Interpretation: This study demonstrated that ATXN7L3 is a novel regulator of SMAD7 transcription, subsequently participating in inhibition of tumor growth in HCC, which provides an insight to support a previously unknown role of ATXN7L3 in HCC progression.
Fund: This work was funded by 973 Program Grant from the Ministry of Science and Technology of China (2013CB945201), National Natural Science Foundation of China (31871286, 81872015, 31701102, 81702800, 81902889), Foundation for Special Professor of Liaoning Province, Natural Science Foundation of Liaoning Province (No.20180530072); China Postdoctoral Science Foundation (2019M651164).

1. Introduction

Liver cancer is the fourth leading cause of cancer death worldwide in 2018 [1]. The most common histological subtype of liver cancer is referred to hepatocellular carcinoma (HCC), which is accounting for 75–85% of all liver cancers [1]. There is an unmet need for the pharmacological therapy for HCC. Sorafenib was the only first line medical therapy for patients with HCC for quite a long time [2]. In recent years, even though encouraging studies have

emerged, such as the kinase inhibitors lenvatinib [3], cabozantinib [4] and regorafenib [5], but they produced only limited beneficial effects, thus other involved molecular mechanisms are still need to be further investigated.

Targeted deubiquitylation of histones is linked to transcription activation, epigenetic regulation and cancer progression [6]. Precise regulation of gene expression programs is established by transcription factors and the recruited coactivators, which are multiprotein complexes enabling histone modification and nucleosome remodeling. ATXN7L3, acting as an adaptor protein, orchestrates activities of multiple deubiquitinating enzymes and acts as a global facilitator for H2B deubiquitination which is closely linked to transcription regulation [7,8].

Research in context

Evidence before this study

Hepatocellular carcinoma (HCC) is a leading cause of cancer death worldwide with unmet need for the pharmacological therapy, thus the involved molecular mechanisms are still need to be further investigated. ATXN7L3 orchestrates activities of multiple deubiquitinating enzymes and acts as a global facilitator for H2B deubiquitination, but the functions of ATXN7L3 in HCC progression are not known.

Added value of this study

This study demonstrated that ATXN7L3 positively regulates the transcription of *SMAD7*. ATXN7L3 associates with estrogen receptor α (ERα), and functions as a coactivator for ERα-mediated transactivation in HCC cells, thereby contributing to enhancement of SMAD7 transcription. ATXN7L3 is recruited to the promoter regions of *SMAD7* gene, thereby regulating histone H2B ubiquitination level, to enhance *SMAD7* transcription. We further globally identified a series of genes regulated by ATXN7L3. Moreover, ATXN7L3 participates in suppression of tumor growth *in vitro* and *in vivo*. In addition, ATXN7L3 is lower expressed in HCC samples, which is correlated with the expression of SMAD7 in HCC tissues. And the expression of ATXN7L3 negatively correlates with poor clinical outcome in patients with HCC.

Implication of all the available evidence

This study demonstrated that ATXN7L3 is a novel regulator of SMAD7 transcription, subsequently participating in inhibition of tumor growth in HCC, which provides an insight to support a previously unknown role of ATXN7L3 in suppression of HCC progression.

ATXN7L3 (Sgf11 in yeast) was named based on its homology to ATXN7 (Sgf73 in yeast), and was first described as another subunit of the human Spt−Ada−Gcn5−acetyltransferase (hSAGA) complex along with ATXN7 [9]. SAGA complex is the first isolated multisubunit complex, which is evolutionarily conserved from yeast to humans [10]. This complex contains both house histone acetyltransferase (HAT) activity and deubiquitination activity, which are mediated by the catalytic activity of GCN5 subunit and deubiquitination module (DUBm), respectively [11−13]. Yeast SAGA complex contains the ubiquitin-specific protease yUbp8, which was shown to remove ubiquitin from monoubiquitinated Lysine 120 of histone H2B (H2BK120ub1, hereafter abbreviated as H2Bub1)[14, 15]. Similar enzymatic activity is carried out by ubiquitin-specific protease 22 (USP22) in hSAGA complex [12,16]. ATXN7L3, along with ENY2 and USP22, form the DUBm of hSAGA. This DUBm of hSAGA can efficiently remove ubiquitin both from histone H2A and H2B *in vitro*, whereas is directed against H2Bub and to a lesser extent H2Aub *in vivo* [12,13]. ATXN7 anchors the DUB module to the larger SAGA complex [17]. Nevertheless, DUBm can bind to chromatin and regulate transcription independently of the SAGA complex [18]. In addition, ATXN7L3 and ENY2, acting as adaptor proteins, also form deubiquitinating complex on histone H2B with USP27X and USP51, which is independently of the SAGA complex [7]. Till now, the functions of ATXN7L3 in HCC progression are not known.

SMAD7 is the endogenous negative regulator of TGF-β signal pathway and acts as a tumor suppressor in HCC [19−22]. SMAD7 expression is down-regulated in HCC [21]. High level of SMAD7 expression is correlation with better clinical outcome in patients

with HCC [20]. In mice, hepatocyte-specific Smad7 deletion accelerates DEN-induced HCC via activation of signal transducer and activator of transcription factor 3 (STAT3) signaling and TGF-β signaling, accompanied by reduced p21 and upregulated c-Myc expression in the tumors [20]. SMAD7 suppresses HCC cell growth by inhibiting proliferation and G1-S phase transition, as well as inducing apoptosis through attenuation of NF-κB and TGFβ signaling [22]. Further, down-regulated expression of SMAD7 is involved in drug resistance and recurrence of HCC [21]. Previous research reported that KLF4 suppresses oncogenic TGF-β signaling by activation of SMAD7 transcription, and loss of KLF4 expression may contribute to activation of oncogenic TGF-β signaling and subsequent tumor progression in primary HCC [23]. But more details involved in regulation of SMAD7 transcription still need to be investigated.

In this study, we found that ATXN7L3 positively regulates the transcription of SMAD7. Further, ATXN7L3 associates with estrogen receptor α (ERα) and functions as a coactivator for ERα-mediated transactivation in HCC cells. ATXN7L3 is recruited to the promoter regions of *SMAD7* gene, thereby regulating histone H2B ubiquitination level, to be involved in upregulation of *SMAD7* transcription. We further globally identified a series of genes regulated by ATXN7L3. Moreover, the results showed that ATXN7L3 participates in suppression of tumor growth *in vitro* and *in vivo*. In addition, ATXN7L3 is lower expressed in HCC samples, which is correlated with the expression of SMAD7 in HCC tissues. And the expression of ATXN7L3 negatively correlates with clinical outcome in patients with HCC. Our study provides compelling evidence that ATXN7L3 functions on modulation of SMAD7 transcription and suppression of HCC progression. Thus, ATXN7L3 may contribute to potential therapeutic implications in HCC.

2. Material and methods

2.1. Cell culture

Human HCC cell lines were identified using PCR-STR analysis. HepG2 cells were cultured in Minimum Essential Media (Gibco, Cat#415-018), while HCCLM3, Huh7, SMMC7721 and PLC/PRF/5 cells were cultured in Dulbecco's modified Eagle medium (Gibco, Cat#12800-082), and supplemented with 10% (v/v) fetal bovine serum (FBS) (CLARK, Cat#FB15015). Cells were incubated at 37 °C in a humidified incubator containing 5% CO2.

2.2. Antibodies

The antibodies used in this study were: anti-ATXN7L3 (Bethyl, Cat#A302-800A), anti-ERα (Cell Signaling Technology, Cat# 8644), anti-FLAG (Shanghai Genomics, Cat#GNI4110-FG), anti-SMAD7 (Sigma Aldrich, Cat#SAB4200346), anti-H3K4me3 (Sigma-Aldrich, Cat#05-745R), anti-Ub-H2B K120 (Cell Signaling Technology, Cat#5546), anti-SHP1 (ZEN BIO, Cat#501836), annti-phospho-SMAD2 (Ser465/Ser467) (Cell Signaling Technology, Cat#18338), anti-GAPDH (ABclonal, Cat#AC033).

2.3. siRNA and lentiviral production

For RNA interference (RNAi), the chemically synthesized small interfering RNAs (siRNA) of ATXN7L3 were purchased from Sigma Aldrich. The sequences of siRNAs targeting ATXN7L3 were: 1# 5'-GUCUGUGUGCAGAAUCUUA-3', 2# 5'-GCUACUUCUUCUUGGACGA-3', 3# 5'-GUCGAGAGCUCCCUGGAUA-3'. The sequence of negative control siRNA (siCtrl) was 5'- UUCUCCGAACGUGUCACGUTT -3'. And siRNA against ERα were purchased from Dharmacon (Cat#L-003401-00-0005). For lentivirus-delivered RNAi, lentiviral productions were purchased from Shanghai GeneChem Company.

2.4. Immunofluorescence stain

Cells were fixed in 4% paraformaldehyde for 15 min and blocked in 1% donkey serum albumin for 1 hr at room temperature. Then cells were incubated with primary antibody overnight at 4 °C and subsequently FITC or Cy3-conjugated secondary antibody (Jackson Immunoresearch Laboratories Inc, Cat#JAC-711-095-152, JAC-711-165-152). Nuclei were stained with DAPI (Roche, Cat# 10236276001). Respective images were taken under confocal microscopy (Nikon).

2.5. Transfections and dual-luciferase reporter assays

Transfections of plasmids and siRNAs were performed according to manufacturer's instructions of jetPRIME reagents (Polyplus-transfection, Cat# 22Y0302M7). In dual-luciferase reporter assays, cells were co-transfected with the listed constructs and then harvested and lysed in passive lysis buffer after 24 h. Luciferase activities were analyzed by Promega dual-luciferase reporter assay system (Cat#E1910) using GloMax Multi Jr detection system. Firefly luciferase activity was normalized to the activity of Renilla luciferase control. Data represent the mean ± SD from three experiments.

2.6. Total RNA extraction, reverse transcription and quantitative real-time PCR

Total RNA was extracted using TRIzol reagent (Thermo Fisher Scientific, Cat#15596018). cDNA synthesis was carried out with PrimeScript RT reagent Kit with gDNA Eraser (TaKaRa, Cat#RR047A), and then analyzed using SYBR Green in Roche LightCycler96 system according to the manufacturer's instructions. Sequence of primers were listed in Supplementary Table S1.

2.7. Co-immunoprecipitation (Co-IP) and Western blot

For Co-IP, the whole cell lysates were extracted and equal protein amounts were immunoprecipitated with specific antibody or control IgG. And immune complexes were analyzed by western blot.

2.8. GST pull-down

GST pull-down have been described previously [24]. GST, or GST-fusion proteins (GST-ERα 29-180 aa and GST-ERα 282-595 aa) coupled with glutathione-Sepharose beads were incubated with *in vitro* transcripted and translated FLAG-ATXN7L3. The binding proteins were detected by western blot and stained by Coomassie Brilliant Blue dye.

2.9. Chromatin Immunoprecipitation (ChIP)

ChIP experiment was performed as previously described [25]. Briefly, cells were cross-linked with 1% formaldehyde and then were lysed with lysis buffer and sonicated on ice. Sonicated chromatin solutions were incubated with indicated antibodies at 4 °C overnight and subsequently incubated with protein A-sepharose for 4 h. Then immunoprecipitated complex were washed sequentially with low salt buffer, high salt buffer, LiCl buffer and TE buffer. The protein-DNA complexes were eluted and the crosslinking was reversed. The purified DNA was resuspended in TE buffer and then amplified by real-time PCR. Sequence of primers were listed in Supplementary Table S2.

2.10. RNA sequencing data and analysis

RNA sequencing was accomplished in Wuhan SeqHealth Technology Company. Cells with lentivirus-mediated knockdown of ATXN7L3 (shATXN7L3) and the negative control (shCtrl) were harvested, and performed to RNA extraction using TRIzol (Invitrogen, Cat#15596026). Qualified RNAs were subjected to library preparation, and the library products corresponding to 200−500 bps were enriched, quantified and finally sequenced on Hiseq X 10 sequencer (Illumina). All RNA sequencing data have been submitted to GEO datasets: GSE157110.

2.11. Cell growth analysis and colony formation assay

For cell viability assay, 2×10^3 cells were plated in 96-well plates, and measured using MTS assay (Promega, Cat#G3580) with the absorbance at 490 nm at the indicated times in medium with 10% CSS supplemented with 10^{-7} M E2 or ethanol vehicle. For growth curve analysis, cells were plated at a density of 1×10^4 cells per well. Cells were trypsinized and counted using a hemocytometer every two day. For colony formation assay, 1×10^3 cells were maintained in medium for 7 days, then cells were fixed with 4% paraformaldehyde and stained with Coomassie brilliant blue dye.

2.12. Xenograft tumor growth

Animal work was carried out under the supervision and guidelines of the China Medical University of Animal Care Center in compliance with the ethical regulations approved by the Animal Ethics Committee of China Medical University. 1.0×10^6 cells were suspended in $100 \mu l$ medium with half Metrigel (BD Biosciences) and injected subcutaneously into the 5-week-old male BALB/C-nude mice. Tumors was measured every two days using an electronic caliper and tumor volume was calculated according to the formula $0.5 \times width^2 \times length$. 12 days after inoculation, mice were sacrificed following the policy of the humane treatment of tumor bearing animals. No animals suffered unnecessarily during the experiment.

2.13. Patients and specimens

149 HCC specimens, 28 fresh HCC tissues and the matched adjacent noncancerous liver tissues were obtained from patients who received hepatectomy at the first affiliated hospital China medical university. The collection of samples was approved by the Medical Ethics Committee of China Medical University, and the informed consents of the patients were obtained.

2.14. Immunohistochemical (IHC) analysis

IHC experiment was performed as previously described [24]. Tissue sections were dewaxed, rehydrated, removed endogenous peroxidase, boiled for antigen retrieval, followed by incubation with indicated antibodies and streptavidin-perosidase-conjugated second antibodies (Maixin Biotech. Co., Ltd.). The signals were visualized with diaminobenzidine and the nuclei were counterstained with hematoxylin.

The stained sections were evaluated by H score method, which assigned the score based on the percentage of cells stained at different intensities. The final H score, which ranged from 0 to 3, was determined by summing the percentage of positive-staining cells (0-100%) at each intensity multiplied by the corresponding staining intensity (0-3).

2.15. Statistics

All data were analyzed using SPSS statistical software program. For real-time PCR, luciferase assay and cell growth assay, two-sided Student's *t*-test was used to determinate the significant difference. For IHC, chi-square test was used to determinate the significant difference between immunohistochemical expression of ATXN7L3 and clinicopathological factors.

3. Results

3.1. ATXN7L3 positively regulated the transcription of SMAD7

In order to determine whether ATXN7L3 play a role in regulation of SMAD7 transcription, we performed a pairwise gene correlation analysis in TCGA database using the Gene Expression Profiling Interactive Analysis (GEPIA) [26]. And a strong positive correlation was established between the mRNA level of *ATXN7L3* and that of *SMAD7* in HCC samples (Fig. 1a). To further confirm the correlation between *ATXN7L3* and *SMAD7*, siRNAs targeting 3 different sequences of *ATXN7L3* were transfected into HCCLM3 cells, and they led to obvious reductions of ATXN7L3 mRNA and protein expressions (Fig. 1b and 1c). Accompanied with knockdown of ATXN7L3, the mRNA and protein levels of SMAD7 significantly decreased (Fig. 1b and 1c). In addition, ectopic expression of ATXN7L3 increased SMAD7 expression (Fig. 1d). In line with previously published data, knockdown of ATXN7L3 induced a robust increase of H2Bub1 (Fig. 1c), and overexpression of ATXN7L3 decreased H2Bub1 levels (Fig. 1d). These data suggested that ATXN7L3 positively regulated the transcription of *SMAD7*.

3.2. ATXN7L3 associated with estrogen receptor α (ERα) and functioned as a coactivator for ERα-mediated transactivation in HCC cells

Then, we wanted to elucidate the potential mechanism involved in ATXN7L3-mediated transactivation of SMAD7. We asked whether ATXN7L3 could interact with KLF4, which functions in the activation of SMAD7 transcription in HCC [23], but no visible interaction between ATXN7L3 and KLF4 was detected (Supplementary Figure S1). Previous research reported that SMAD7 is an estrogen-induced gene in MCF7 cells [27]. It has also been shown that ATXN7L3 can function as a coactivator for androgen receptor (AR)-mediated transactivation [12]. As ERα is another hormone receptor as well as the major receptor of estrogen, we hypothesized ATXN7L3 may serve as a co-regulator of ERα. We then examined the endogenous protein expressions of ATXN7L3 and ERα in five cultured HCC cell lines, including HCCLM3, Huh7, HepG2, SMMC-7721 and PLC/PRF/5. In agreement with previous reports [7], the expression levels of ATXN7L3 are normally limiting in those cells, while HCCLM3 cells expressed higher level of ATXN7L3 (Supplementary Figure S2).

Further, we analyzed putative interactions between ATXN7L3 and ERα. By Co-IP, we confirmed the interaction between exogenous
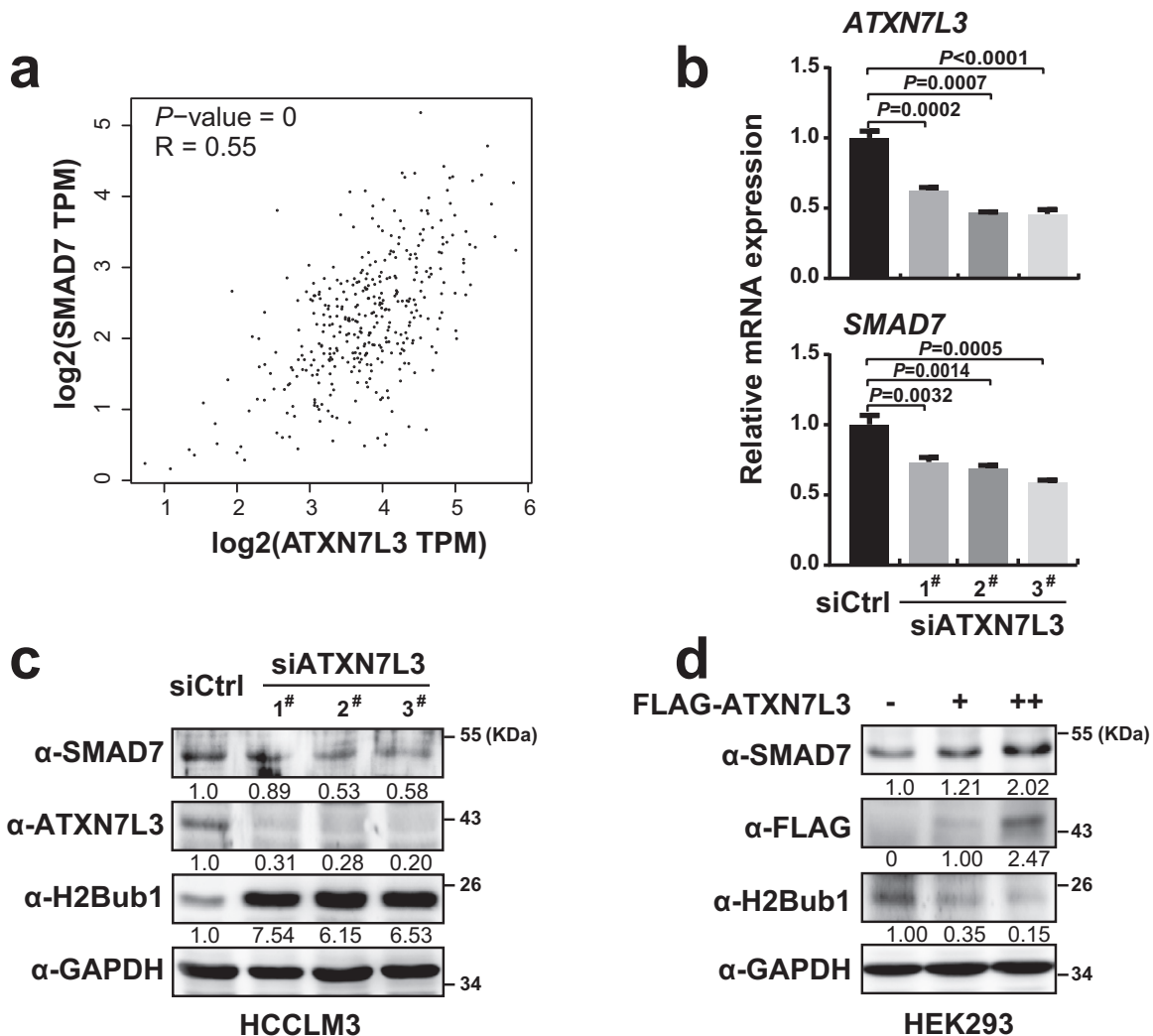

Fig. 1. ATXN7L3 positively regulates SMAD7 transcription. **(a)** The mRNA expression of *ATXN7L3* is positively correlated with that of *SMAD7* in TCGA database. The relative level of *ATXN7L3* was plotted against that of *SMAD7*. **(b)** Knockdown of ATXN7L3 downregulated mRNA expression of *SMAD7*. HCCLM3 cells were transfected with siCtrl or siATXN7L3. After 48 hr, cells were collected for RNA extraction and quantitative real-time PCR were performed. Data represents the mean ± SD of triplicate real-time PCR. **(c)** Knockdown of ATXN7L3 downregulated protein expression of SMAD7. HCCLM3 cells were transfected with siCtrl or siATXN7L3. After 48 hr, cells were collected for protein extraction and subjected to western blot analysis using indicated antibodies. The results were quantified through Image J software and GAPDH was used as internal control. **(d)** Ectopic expression of ATXN7L3 upregulated protein expression of SMAD7. HCCLM3 cells were transfected with ATXN7L3-expressing plasmids with different doses or control vector. After 24 hr, cells were collected for protein extraction and subjected to western blot analysis using indicated antibodies. The results were quantified through Image J software and GAPDH was used as internal control.

ATXN7L3 and ERα, both in the absence and presence of estrogen (E2) (Fig. 2a). And the interaction between endogenous ATXN7L3 and ERα could be observed in HCCLM3 cells, too (Fig. 2b and 2c). Moreover, the results of immunofluorescence experiments showed that exogenous ATXN7L3 was compartmentalized in the nucleus with ERα (Fig. 2d). And a direct interaction between ATXN7L3 and ERα 282-585 aa was confirmed by *in vitro* GST pull-down (Fig. 2e). In addition, USP22 can also be detected after an ATXN7L3 immunoprecipitation in HCC cells, revealing normal incorporation of DUBm subunits in HCCLM3 cells (Supplementary Figure S3). Taken together, these results indicated that ATXN7L3 physically associates with ERα in HCC cells.

We next asked whether ATXN7L3 can play a role in ERα-mediated transcription. We then performed dual-reporter system analysis harboring an estrogen response element-luciferase (ERE-luc) reporter gene to examine ERα-mediated transactivation. As shown in Fig. 2f and 2g, E2 treatment induced ERα-mediated transactivation, and ATXN7L3 further enhanced ERα-mediated transactivation significantly, in HEK293 cells and HepG2 cells. Furthermore, knockdown of ATXN7L3 impressed ERα-mediated transactivation significantly in HCCLM3 cells (Fig. 2h). These results together with the observed interaction between ATXN7L3 and ERα suggested that ATXN7L3 functions as a coactivator for ERα-mediated transactivation.

3.3. ATXN7L3 coactivates ERα-mediated transactivation of SMAD7

Having established that ATXN7L3 is a coactivator for ERα, we then analyzed the effects of ATXN7L3 on ERα-dependent gene activation. Indeed, E2 treatment induced the mRNA expression of two well-characterized ERα-target genes, *SMAD7* and *SHP1* (Fig. 3a). Transient ATXN7L3 knockdown by siRNA significantly attenuated mRNA expression of *SMAD7* both in the absence and presence of ligand, while the that of *SHP1* was non-significantly changed (Fig. 3a). Moreover, knockdown of ATXN7L3 led to obvious reductions of SMAD7 protein levels (Fig. 3b), While overexpression of ATXN7L3 increased protein expression of SMAD7 (Fig. 3c). In contrast, no obvious effects on SHP1 or ERα protein expression had been observed after ATXN7L3 knockdown or overexpression (Fig. 3a-3c). In addition, knockdown of ERα attenuated exogenous ATXN7L3-mediated expression of *SMAD7*, indicating the enhancement of *SMAD7* expression by ATXN7L3 is associated with ERα (Fig. 3d).

It was reported that ERα binds on distal enhancers of *SMAD7* gene with JMJD6, which is required for RNA polymerase II recruitment and enhancer RNA production, resulting in transcriptional pause release of SMAD7 in MCF7 cells [27]. We then focused on the proximal region of *SMAD7* gene. Bioinformatics analysis identified three putative ERα binding cis elements (referred to as ERE1, ERE2 and ERE3) in the proximal region of *SMAD7* (Fig. 3e). To evaluated the suggesting cooperation between ATXN7L3 and ERα, HCCLM3 cells were treated with or without E2 and subjected to chromatin immunoprecipitation (ChIP) to identify recruitment of the two protein on those elements. On ERE1 and ERE2 sites, the enrichment of ATXN7L3 and ERα were limited (Fig. 3f). The highest recruitments of ERα were observed on ERE3, where ATXN7L3 was recruited simultaneously, and their recruitments were significantly increased after E2 addition (Fig. 3g). In addition, knockdown of ATXN7L3 by lentivirus expressing anti-ATXN7L3 siRNA (shATXN7L3, the same target sequence as siRNA3[#]) resulted in accumulation of H2Bub1 and decreased levels of H3K4me3, which have both been linked to transcription activation (Fig. 3g). These data suggested that ATXN7L3 co-activates ERα to regulate transactivation of *SMAD7* at the proximal region, and ATXN7L3 regulates *SMAD7* transcription, at least in part, through interaction with ERα.

3.4. Global identification of target genes regulated by ATXN7L3

We then wanted to identify target genes of ATXN7L3 by global genome-wide analysis. To this end, RNA-sequencing was performed with HCCLM3 cells carrying shATXN7L3 and its control cells (shCtrl). A total of 3831 genes were significantly changed after ATXN7L3 knockdown (P<0.01). There were 1914 ATXN7L3 positive-regulated differentially expressed genes (DEGs), which were significantly downregulated in ATXN7L3 knockdown cells. And 1917 gene were negative-regulated DEGs by ATXN7L3, which were significantly upregulated in ATXN7L3 knockdown cells. In accordance with the co-activation function of ATXN7L3 on ERα-mediated transactivation, a portion of the significant DEGs were known ERα target genes [28] besides *SMAD7*, including *THBS1, IGFBP4, CTSD, SIAH2, JAK1, STC2, CCNG2, NDRG1* and *CRABP2*.

We then focused on top DEGs using ±0.8-log2(fold change) as a cutoff, which were 246 positive-regulated DEGs and 187 negative-regulated DEGs (Fig. 4a and 4b, listed in Supplementary Table S3). Pathway and process enrichment analysis revealed that the identified genes appeared to involve broad functions and multiple pathways, including cell-cell adhesion, multicellular organismal homeostasis, signaling by nuclear receptors, and so on (Fig. 4c). It was noteworthy that the top 20 results from 246 ATXN7L3 positive-regulated DEGs included negative regulation of growth, and regulation of growth was involved in top 20 results from 187 ATXN7L3 negative-regulated DEGs (Fig. 4c). We further selected a subset of genes, which are obviously regulated and involved in cell growth regulation (Fig. 4d). Moreover, real-time PCR experiments were performed to confirm the analysis results. The mRNA expression of *NKX2-2, IGFBP5* and *AGT* were decreased after ATXN7L3 knockdown, whereas that of *HMGA2, IL7R, PTSG2*, and *CISH* were increased (Fig. 4e). Together, these data suggested that ATXN7L3 participates in modulation of a portion of endogenous target genes.

3.5. ATXN7L3 is involved in suppression of cell growth in HCC cells

Having established that ATXN7L3 regulated the expression of genes associated with growth control, we next performed a series of experiments to validate its function on cell growth in HCC cells. We first investigated the impact of ATXN7L3 on cell growth in the absence or presence of ligand. In line with previous report that estrogen exerts protective effects against HCC [29], our results showed E2 treatment slightly repressed cell growth of HCCLM3 cells (Fig. 5a). Cell growth with ATXN7L3 knockdown (shATXN7L3) was faster than that with the control (shCtrl), both in the absence and presence of ligand (Fig. 5a). Further, we analyzed the overall function of ATXN7L3 under normal culture condition, and promoted cell proliferation was observed by ATXN7L3 knockdown with growth curves analysis (Supplementary Figure S4). Moreover, knockdown of SMAD7 impaired the growth inhibition by ATXN7L3, indicating that growth inhibition by ATXN7L3 is associated with SMAD7 (Fig. 5b). Colony formation assays indicated the similar results (Fig. 5c). Finally, we performed *in vivo* tumor growth analysis in a mouse xenograft model. In good agreement with our observations *in vitro*, the promoted tumor burden upon ATXN7L3 knockdown was shown, with bigger volumes and faster growth rate (Fig. 5d-5f). In line with the tumor growth curve, the tumor weights of shATXN7L3 cells were significantly higher (Fig. 5g). We then examined the expression and ATXN7L3 and SMAD7 in those xenograft tumors. Consistent with the observations *in vitro*, the mRNA and protein expressions of SMAD7 were downregulated in the shATXN7L3 tumor (Fig. 5h-5k). Since SMAD7 is an essential regulator of TGFβ signaling, we detected the phosphorylation level of SMAD2 in mouse xenografts, which represents the activation of TGFβ signaling. In line with repressed expression of SMAD7, phosphorylation level of SMAD2 were upregulated in the xenografts derived from shATXN7L3 cells (Fig. 5l). Taken together, ATXN7L3 suppresses HCC cell growth both *in vitro* and *in vivo*, at least in part by enhancing SMAD7 transcription.
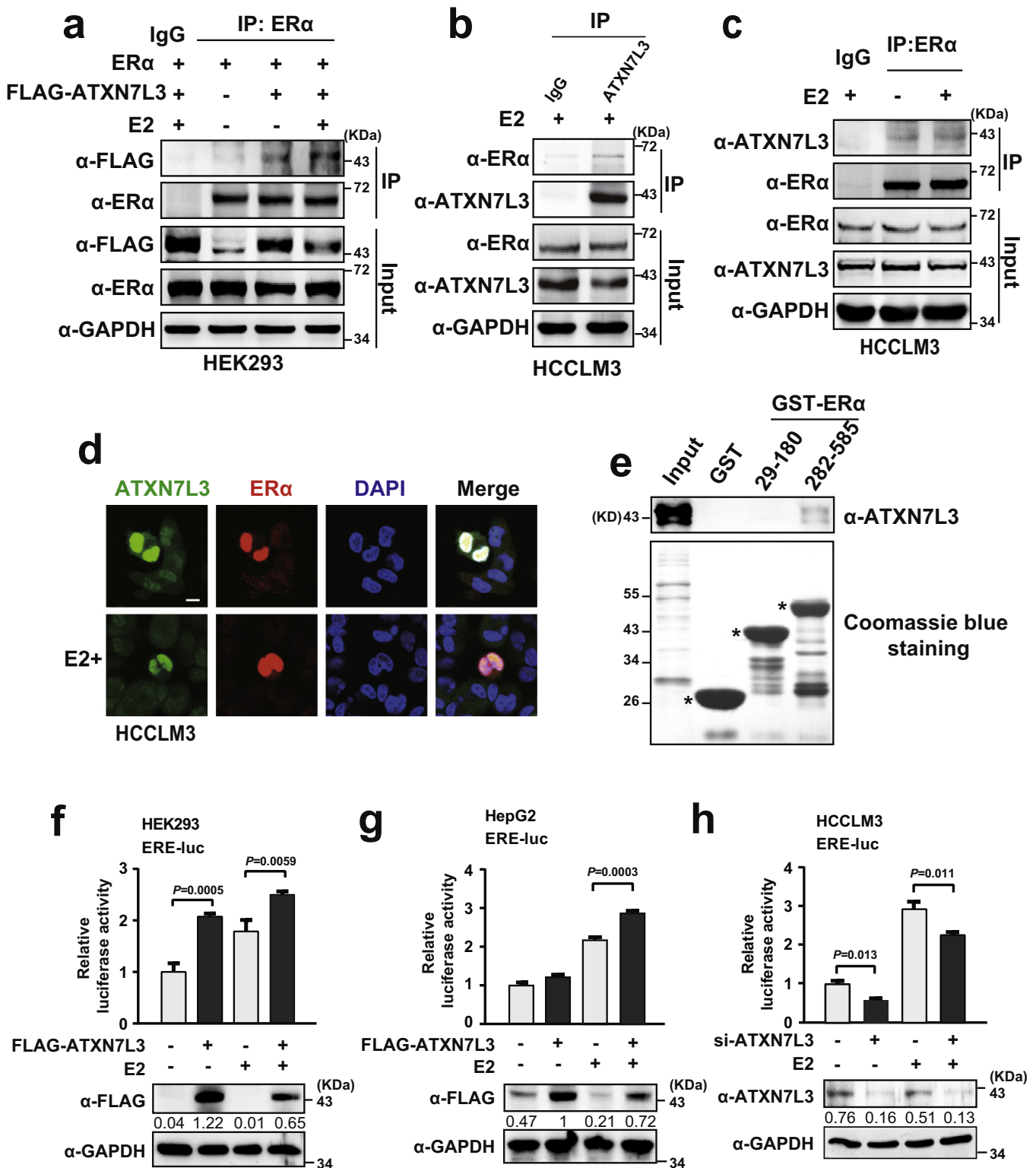
Fig. 2. ATXN7L3 associates with ERα and acts as a coactivator of ERα. (**a**) ATXN7L3 and ERα interacts with each other in HEK293 cells. HEK-293 cells were co-transfected with plasmids expressing ATXN7L3 and ERα. After 24 hr, cells were treated by E2 (10^{-7} M) or ethanol vehicle for 4 hr. Then cells were harvested and equal amounts of cell lysates were subjected to immunoprecipitation with normal IgG, or anti-ERα antibodies. The immunoprecipitated proteins were subjected to western blot analysis using indicated antibodies. (**b-c**) Endogenous ATXN7L3 and ERα interacts with each other in HCCLM3 cells. Upon treatment of 10^{-7} M E2 or ethanol vehicle for 24 hr, cells were harvested and equal amounts of cell lysates were subjected to immunoprecipitation with normal IgG, anti-ATXN7L3 or anti-ERα antibodies. The immunoprecipitated proteins were subjected to western blot analysis using indicated antibodies. (**d**) Subcellular localizations of the ATXN7L3 and ERα. HCCLM3 cells were co-transfected with plasmids expressing ATXN7L3 and ERα. After 10^{-7} M E2 stimulation or ethanol vehicle for 4 hr, HCCLM3 cells were fixed and stained with antibody against ATXN7L3 (green) or ERα (red). DAPI was used to visualize the nucleus (blue). Merged images were shown as indicated. Scale bar, 20 μm. (**e**) Identification of domains in ERα for ATXN7L3 interaction. ATXN7L3 protein was synthesized by transcription and translation kit *in vitro*, then was incubated with GST or GST- ERα deletion mutants. Bound proteins were washed and analyzed by western blot. GST and GST- ERα deletion mutants were stained by Coomassie brilliant blue staining. *, position of GST and GST- ERα deletion mutants. (**f-h**) ATXN7L3 enhances ERα-mediated transactivation. HEK-293 cells (**f**), HepG2 cells (**g**) or HCCLM3 (**h**) were co-transfected with ERE-luc, pRL-TK and ERα, together with the indicated expression plasmids or siRNA in the presence of 10^{-7} M E2 or ethanol vehicle. After 24 hr, cells were lysed and assayed using the dual-luciferase reporter assay system. The expression of ATXN7L3 was evaluated by western blot in lower panel. Error bars represent mean ± SD of three replicates. The western blot results were quantified through Image J software and GAPDH was used as internal control.
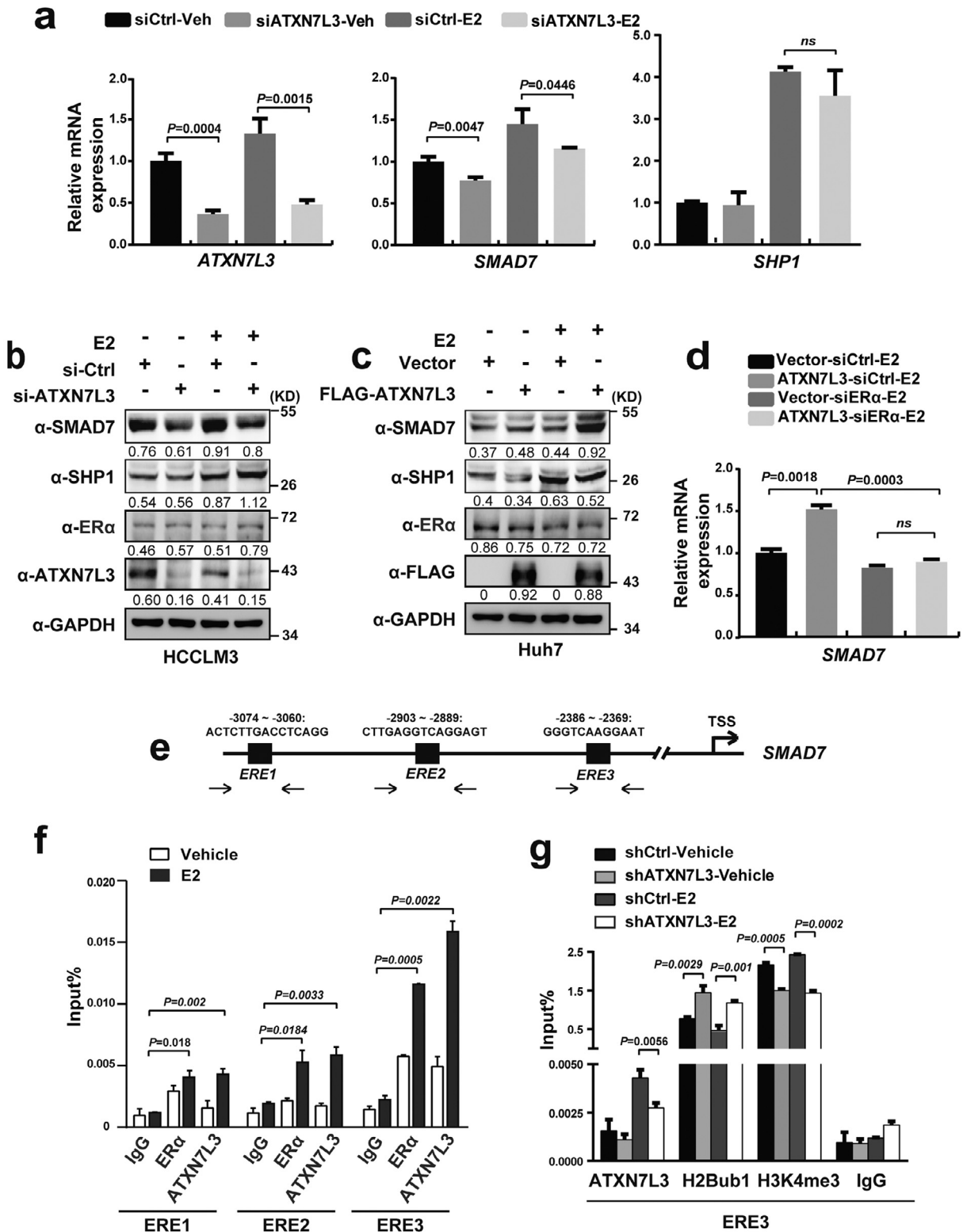
Fig. 3. ATXN7L3 knockdown represses the ERα regulated SMAD7 expression and ATXN7L3 is recruited to ERα-binding regions of SMAD7. (**a**) Effect of ATXN7L3 knockdown on the mRNA expression of *SMAD7* and *SHP1* in HCCLM3 cells. Cells were transfected with siCtrl or siATXN7L3 (3#). After treatment of 10^{-7} M E2 or ethanol vehicle for 24 hr, cells were collected for RNA extraction and quantitative real-time PCR were performed. (**b**) Effect of ATXN7L3 knockdown on the protein expression of SMAD7 and SHP1 in HCCLM3 cells. HCCLM3 cells were transfected with siCtrl or siATXN7L3 (3#). After treatment with 10^{-7} M E2 or ethanol vehicle for 24 hr, cells were harvested for protein extraction. Western blot was performed to detect the expression of proteins as indicated. (**c**) Effect of ATXN7L3 overexpression on the protein expression of SMAD7 and SHP1 in Huh7 cells. Huh7 cells were transfected with plasmid expressing ectopic ATXN7L3 or control vector. After treatment with 10^{-7} M E2 or ethanol vehicle for 24 hr, cells were harvested for protein extraction. Western blot was performed to detect the expression of proteins as indicated. The results were quantified through Image J software and GAPDH was used as internal control. (**d**) The enhancement of *SMAD7* expression by ATXN7L3 is associated with ERα. Huh7 cells were transfected with siCtrl or siERα. In the next day, cells were transfected with ATXN7L3 expressing plasmid or control. After treatment of 10^{-7} M E2 or ethanol vehicle for 24 hr, cells were collected for RNA extraction and quantitative real-time PCR were performed. (**e**) Diagram represents cis-elements in *SMAD7*. (**f**) ATXN7L3 and ERα are recruited to cis-elements in *SMAD7*. After treatment with 10^{-7} M E2 or ethanol for 4 hr, HCCLM3 cells were cross-linked and subjected to ChIP experiments by anti-ATXN7L3, anti-ERα or normal IgG. The precipitated DNA were normalized to input DNA signal as a percentage. Data represents the mean ±SD of triplicate real-time PCR. (**g**) ATXN7L3 knockdown impacts on the epigenetic modification on cis-elements in *SMAD7*. In HCCLM3 cells, lentivirus-mediated knockdown of ATXN7L3 (shATXN7L3) and control cells (shCtrl) were treated with 10^{-7} M E2 or ethanol for 4 hr, then cells were subjected to ChIP assay with antibodies indicated. The precipitated DNA was normalized to input DNA signal as a percentage. Data represents the mean ± SD of triplicate real-time PCR.
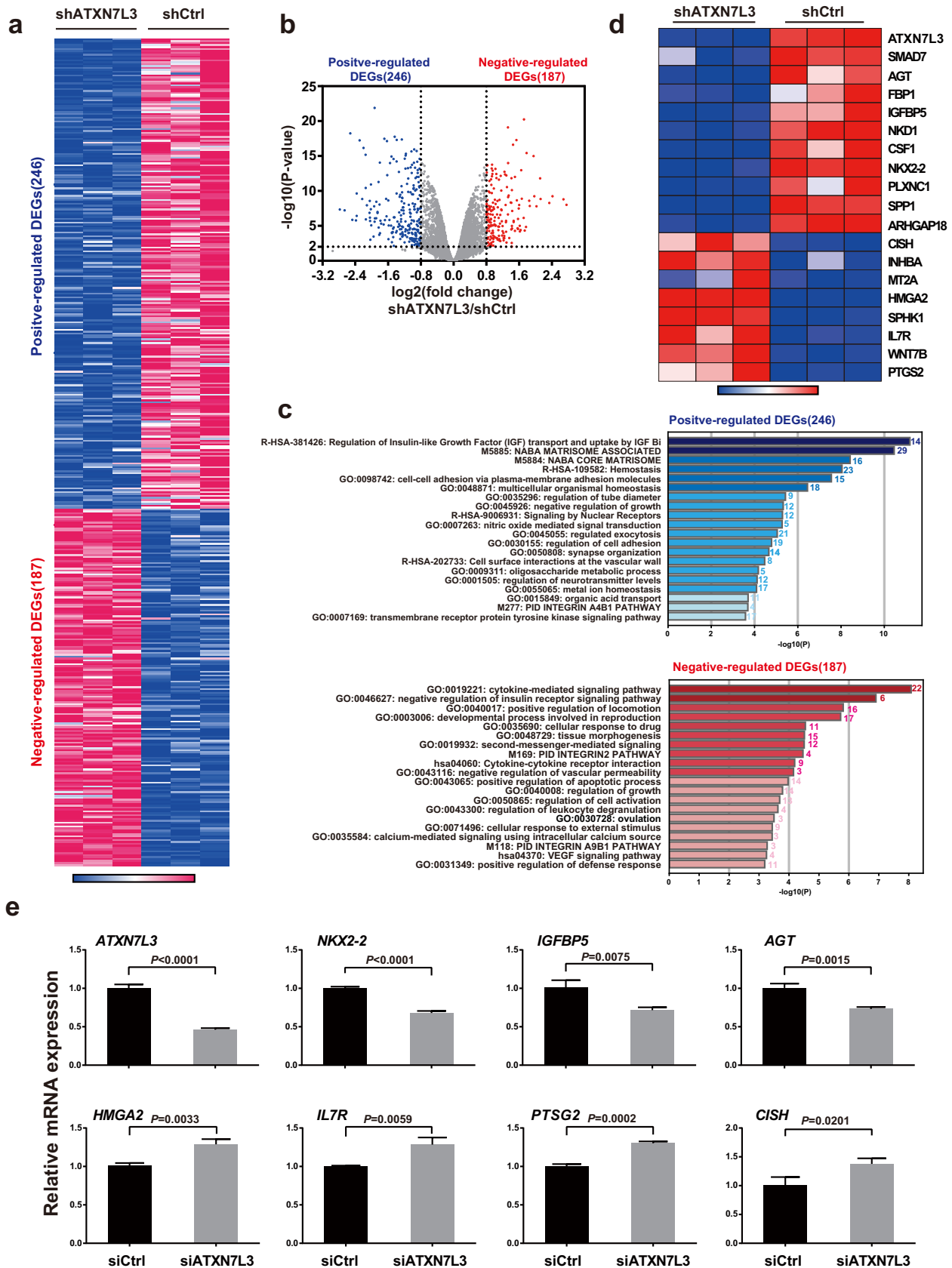
Fig. 4. Identification of target genes regulated by ATXN7L3 with global genome-wide analysis. **(a)** Top genes significantly changed after ATXN7L3 knockdown. Heat map displayed the top genes with altered expression upon ATXN7L3 knockdown. A relative color scheme uses the minimum and maximum values in each row to convert values to colors. **(b)** Val-conoplot shows genes whose expression was significantly changed upon ATXN7L3 knockdown. Blue plots represented more significant positive-affected genes (PAGs) and the red plots for negative-affected genes (NAGs). **(c)** The enriched biological processes of ATXN7L3 regulated genes revealed by GO and KEGG pathway analysis. **(d)** Heat map of the selected genes from (A). **(e)** Evaluation of mRNA expression of the indicated genes after ATXN7L3 knockdown. HCCLM3 cells were transfected with siCtrl or siATXN7L3. After 48 hr, cells were collected for RNA extraction and quantitative real-time PCR were performed. Data represents the mean ± SD of triplicate real-time PCR
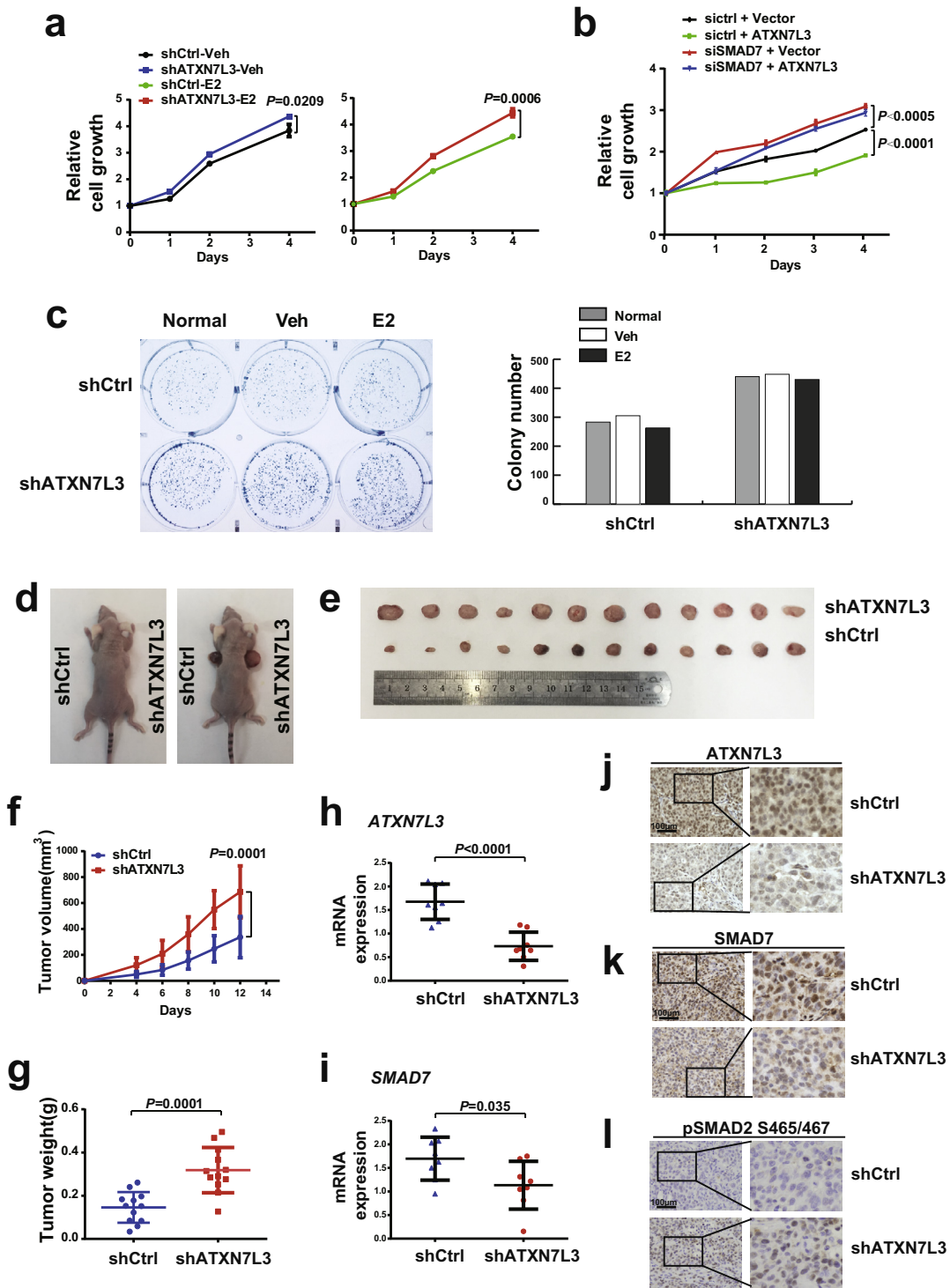
Fig. 5. ATXN7L3 knockdown promotes tumor growth of HCC cells *in vitro* and *in vivo*. (**a**) ATXN7L3 knockdown promotes cell proliferation of HCCLM3 cells. Lentivirus-mediated knockdown of ATXN7L3 (shATXN7L3) in HCCLM3 cells and control cells (shCtrl) were treated with 10^{-7} M E2 or ethanol. After indicated time, MTS reagent was added, then absorbance at 490 nm was measured and normalized to plotted. Points, mean of three replicates; bars, SD. (**b**) ATXN7L3 overexpression represses promotes cell proliferation of HCCLM3 cells, and knockdown of SMAD7 impairs the growth inhibition by ATXN7L3. (**c**) Effects of ATXN7L3 knockdown on the growth of HCCLM3 cells are shown by colony formation assay. Statistical analysis of colony formation assay was shown in the right panel. (**d**) Representative photograph of mice with tumor xenografts. (**e**) Photograph of all xenograft tumors from different groups. (**f**) Tumor volumes of xenografts after injection were shown. Bars represented standard alteration of the mean ± SD. (**g**) Tumor weights of xenografts were shown. (**h** and **i**) Total RNA of xenograft tumors were extracted and the mRNA expression of *ATXN7L3* and *SMAD7* were shown. (**j - l**) Expressions of ATXN7L3, SMAD7 and phospho-SMAD2 Ser465/467 in xenograft tumors were detected by IHC assays.

3.6. Reduced ATXN7L3 and SMAD7 expressions and clinical relevance of ATXN7L3 in human HCC

Having revealed the involvement of ATXN7L3 in SMAD7 transactivation, we next examined the expression of ATXN7L3 and SMAD7 in 28 pairs of HCC tissues and the matched adjacent noncancerous tissues by western blot. ATXN7L3 expression in 21 HCCs (75%) and SMAD7 expression in 23 HCCs (82.14%) were significantly reduced, compared with that in the matched adjacent noncancerous tissues (Fig. 6a and 6b). As shown in Fig. 6c, significant correlation between
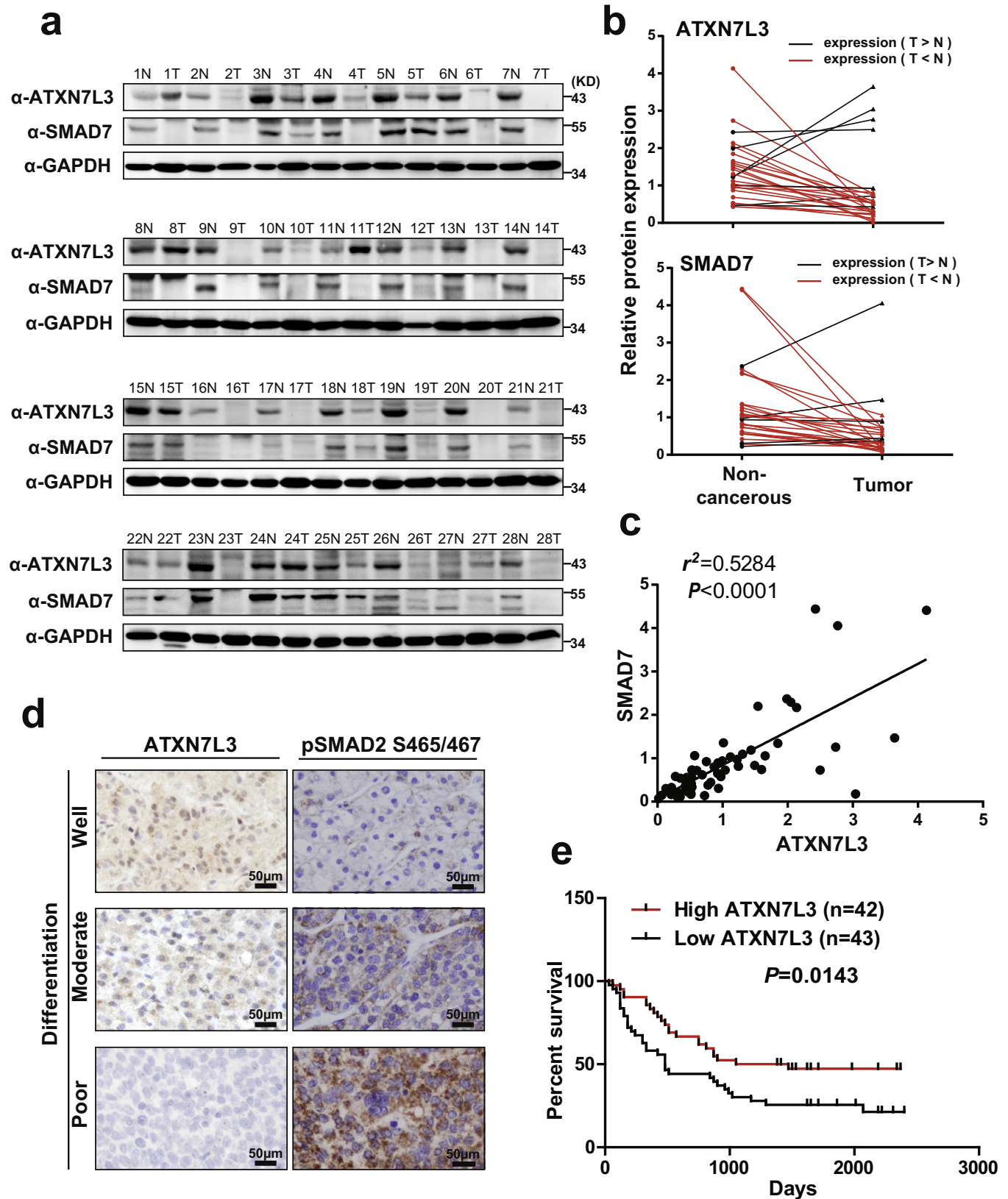
Fig. 6. Expression of ATXN7L3 positively correlates with that of SMAD7 in clinical HCC samples. (**a**) Evaluation of the indicated proteins in clinical HCC tissues the matched adjacent non-cancerous tissues. Lysates of tissues were subjected to western blot analysis. GAPDH was used as the loading control. N, adjacent non-cancerous tissues; T, tumor tissues. (**b**) The expression of ATXN7L3 and SMAD7 is decreased in clinical HCC tissues, compared with the matched adjacent non-cancerous tissues. Data from (A) were quantified by densitometry, with GAPDH as the reference. Black color indicated the cases in which ATXN7L3 or SMAD7 expression were increased in tumor. (**c**) The expression level of ATXN7L3 is positively correlated with SMAD7. Quantified expression levels of ATXN7L3 and SMAD7 from the 28-pair samples were statistically analyzed. The relative level of ATXN7L3 was plotted against that of SMAD7. (**d**) Representative images of ATXN7L3 and phospho-SMAD2 Ser465/467 immunohistochemical staining in HCC cases with different stage of differentiation. (**e**) Lower expression of ATXN7L3 positively correlates with poor clinical outcome in patients with HCC. ATXN7L3 expression in 85 HCC specimens with follow-up information were evaluated by IHC stain. The subjects were divided into two groups based on the median expression score, representing low and high expression. And the overall survival was analyzed by Kaplan−Meier (KM) method.

Table 1
Relation between the clinicopathologic variables and ATXN7L3 expression in HCC

| Variable | cases (n=64) | ATXN7L3 expression | | χ^2 | P value[a] |
		Low	High		
Age (Year)[b]				1	0.317
<52.1	32	14	18		
≥52.1	32	18	14		
Gender				2.003	0.157
Female	17	11	21		
Male	47	6	26		
Differentiation				7.819	0.005*
Well-Moderate	51	21	30		
Poor	13	11	2		
AFP stain				0.366	0.545
Negative	14	8	6		
Positive	50	24	26		

[a] :Chi-square test
[b] :Mean age

the protein expression of ATXN7L3 and that of SMAD7 was observed (r^2=0.5284, P<0.0001). The expression of ATXN7L3 was further examined immunohistochemically in 64 HCC tissues. The correlation between immunohistochemical expression of ATXN7L3 and clinicopathological factors was shown in Table 1. Although no significant association between ATXN7L3 expression and age, gender or AFP expression was observed, higher expression of ATXN7L3 was significantly associated with well differentiation (Fig. 6d). Simultaneously, reduced ATXN7L3 expression was accompanied with increasing phosphorylated-SMAD2 (Fig. 6d). In addition, the expression of lower ATXN7L3 positively correlates with poor clinical outcome in patients with HCC (Fig. 6e). These results suggested that ATXN7L3 might plays a role in suppression of clinical human HCC.

4. Discussion

Here we discovered ATXN7L3 serves as a coactivator of ERα and promotes *SMAD7* transactivation via a mechanism involving histone deubiquitination. We also demonstrated the tumor suppressive role of ATXN7L3 and repressed expression of ATXN7L3 in clinical HCC tissues (Fig. 7).

Monoubiquitination of histone H2B at lysine 120 (H2bub1) is written predominantly by the RING finger complex RNF20-RNF40. In previous studies, both tumor suppressor function and tumor promotor function of H2Bub1 were reported [30–33]. While RNF20 knockdown increases cell migration and promotes cell transformation in human cancer cells, RNF20 and H2Bub1 were thought as tumor suppressors [30]. Another report indicated that RNF20 and H2Bub1 have contrasting roles in distinct breast cancer subtypes through differential regulation of key transcriptional programs, suggesting H2Bub1 is implicated in promoting carcinogenesis in breast cancer [31]. In mixed-lineage leukemia (MLL)-fusion leukemia, RNF20 is required for prolife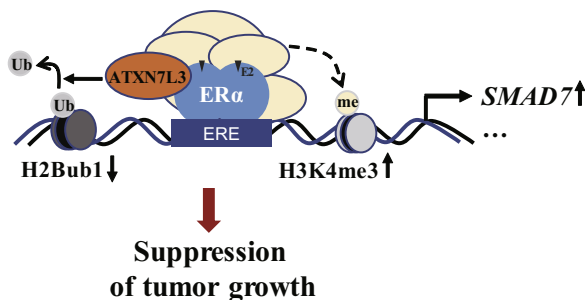ration, and H2Bub1 is enriched within the body of MLL-fusion target genes and promotes their expression [32]. By targeting RNF20 to proteasomal degradation and concomitant loss of H2Bub1, Smad ubiquitin regulatory factor 2 (Smurf2) exhibits tumor suppressor function with controlling chromatin landscape and genome stability [33]. Altogether, the exact role of H2Bub1 in cancer is context-dependent, and depends on particular molecular pathways in the given cancer. Previously published data shows that ATXN7L3 acts as a robust controller for H2B deubiquitination throughout the entire transcribed genome [7,8]. In this study, we also observed a substantial increase in global H2Bub1 levels by ATXN7L3 knockdown (Fig. 1c), and further demonstrate that ATXN7L3 contributes to inhibition of tumor growth in HCC cells and tumor xenografts in mice (Fig. 5). We also detected the interaction between ATXN7L3 and USP22 (Supplementary Figure S3). As USP22 acts as a tumor promoter in HCC [34–36], our data implies ATXN7L3 predominantly functions with other deubiquitinating enzymes, which may serve as tumor suppressors in HCC and should be identified in future work.

Canonical estrogen signaling is mediated through ERα, resulting in transcriptional target gene activation and play a suppressing role in HCC [29,37–43]. Estrogen has been proven to exert protective effects against HCC through IL-6 restrictions, STAT3 inactivation and tumor-associated macrophage inhibition [37–39]. Further, ERα was identified as a candidate tumor suppressor gene in HCC [40]. ERα interacts with and alters binding of HNF-4α to the HBV enhancer I, then prevents activation of HBV transcription [41]. ERα over-expression mediated apoptosis by binding with SP1 proteins in HCC Hep3B cells [29]. In addition, repressed ERα function contributes to HCC progression. MicroRNA-18a prevents ERα expression, promoting proliferation of HCC cells [42]. Elevated expression of Erbin in HCC promotes tumorigenes by promoting Chip binding and ubiquitination ERα [43].

In this study, we demonstrated ATXN7L3 interacted and co-activated ERα in HCC cells (Fig. 2). ATXN7L3 and ERα were recruited at the proximal region of *SMAD7* gene, and ATXN7L3 knockdown induced accumulation of H2Bub1 at the region (Fig. 3). Besides *SMAD7*, ATXN7L3 also impacted a subset of known ERα target genes (Fig. 4). As reported previously, H2Bub1 is conserved in all eukaryotes and is centrally involved in gene regulation. Histone H2B ubiquitylation and its deubiquitylation are both involved in gene activation [8,17,44,45]. During transcription, H2Bub1 seems to be a highly dynamic process, and the dynamics of H2B ubiquitination and deubiquitination at promoters or transcribed regions are differentially regulated [13,15]. In mammalian cells, H2B ubiquitination is intimately linked with global transcriptional elongation [17]. In human cells, deubiquitination activity of hSAGA complex is required for activator-driven transcription, including AR and c-Myc [12,16]. Another hand, in breast cancer, estrogen-dependent gene transcription relies upon H2Bub1 [46], and SUPT6H is required for ERα activity possibly in part through interaction with RNF40 and regulation of H2Bub1 [47]. Taken together, our findings imply that ATXN7L3, a coactivator of ERα, was involved in ERα-mediated transactivation and the regulation of a subset of endogenous ERα target genes via modulation of H2Bub1, which provides a previously unknown mechanism in ERα activity control in HCC. Therefore, the tumor suppressive role of ATXN7L3 could in part be attributed to ERα activity control and SMAD7 transactivation.

Previous studies reported that ERα interacts with E3 ubiquitin ligases to be degraded with the treatment of E2 [48–50]. It is unexpected that ATXN7L3 protein is reduced by E2 treatment in our data (Fig. 2 and 3). Although the detailed molecular mechanisms for this remains unclear, one possible underlying mechanism is that, the interaction of ATXN7L3 and ERα might influence the E3 ligase induced degradation of ATXN7L3.

It is reported that only a subset of genes was transcriptionally affected by H2Bub1, while H2B ubiquitylation is broadly associated with transcribed genes [30]. In an attempt to define global ATXN7L3

Fig. 7. Schematic representation of ATXN7L3 functions on SMAD7 transactivation and suppression of tumor growth in HCC.

target genes, we used RNA-sequencing in this study. In addition to its role in modulating ERα-mediated transcription, ATXN7L3 also regulated a subset of genes involved in a variety of biological functions (Fig. 4). According the readout gave both ATXN7L3 direct and indirect target genes. It is need to identify the global binding of ATXN7L3 *in vivo*, which will be the subject of further investigation.

Signal-dependent activation by sequence-specific transcription activators would recruit SAGA complex to remove ubiquitin from histones, then collaborates with other complexes, such as MLL complexes and PRC complex, to maintain gene expression programs via epigenetic mechanisms [51]. In line with previous report, the results of ChIP assays from our research (Fig. 3f) showed that ATXN7L3 knockdown decreased H3K4me3 level on cis-element of *SMAD7* along with H2Bub1 changes, indicating that other histone modification enzymes cooperate with ATXN7L3 in transcriptional regulation.

Taken together, our study demonstrated that ATXN7L3 is a novel regulator of SMAD7 transcription with growth inhibitory function in HCC, which provides an insight to support a previously unknown role of ATXN7L3 in tumor progression and a better understanding of the key mechanisms responsible for HCC progression.

Contributors

Ning Sun, Xinping Zhong, Shengli Wang, Kai Zeng, Hongmiao Sun and Ge Sun performed experiments and analyzed the data; Renlong Zou, Wei Liu, Wensu Liu, and Lin Lin, conducted bioinformatic analyses and statistical analyses; Huijuan Song and Chi Lv and Chunyu Wang designed the study and wrote the manuscript; Yue Zhao wrote and revised manuscript. All authors read and approved the final manuscript.

Declaration of Competing Interest

The authors declare no conflict of interests.

Acknowledgements

Funding sources

Supplementary materials

Supplementary material associated with this article can be found, in the online version, at doi:10.1016/j.ebiom.2020.103108.

References

[1] Bray F, Ferlay J, Soerjomataram I, Siegel RL, Torre LA, Jemal A. Global cancer statistics 2018: GLOBOCAN estimates of incidence and mortality worldwide for 36 cancers in 185 countries. CA 2018;68(6):394–424.

[2] Anstee QM, Reeves HL, Kotsiliti E, Govaere O, Heikenwalder M. From NASH to HCC: current concepts and future challenges. Nat Rev Gastroenterol Hepatol 2019;16(7):411–28.

[3] Kudo M. Lenvatinib in advanced hepatocellular carcinoma. Liver Cancer 2017;6 (4):253–63.

[4] Abou-Alfa GK, Meyer T, Cheng AL, El-Khoueiry AB, Rimassa L, Ryoo BY, et al. Cabozantinib in patients with advanced and progressing hepatocellular carcinoma. N Engl J Med 2018;379(1):54–63.

[5] Bruix J, Qin S, Merle P, Granito A, Huang YH, Bodoky G, et al. Regorafenib for patients with hepatocellular carcinoma who progressed on sorafenib treatment (RESORCE): a randomised, double-blind, placebo-controlled, phase 3 trial. Lancet 2017;389(10064):56–66.

[6] Yang S, Yang L, Li X, Li B, Li Y, Zhang X, et al. New insights into autophagy in hepatocellular carcinoma: mechanisms and therapeutic strategies. Am J Cancer Res 2019;9(7):1329–53.

[7] Atanassov BS, Mohan RD, Lan X, Kuang X, Lu Y, Lin K, et al. ATXN7L3 and ENY2 coordinate activity of multiple H2B deubiquitinases important for cellular proliferation and tumor growth. Mol Cell 2016;62(4):558–71.

[8] Bonnet J, Wang CY, Baptista T, Vincent SD, Hsiao WC, Stierle M, et al. The SAGA coactivator complex acts on the whole transcribed genome and is required for RNA polymerase II transcription. Genes Dev 2014;28(18):1999–2012.

[9] Helmlinger D, Hardy S, Sasorith S, Klein F, Robert F, Weber C, et al. Ataxin-7 is a subunit of GCN5 histone acetyltransferase-containing complexes. Hum Mol Genet 2004;13(12):1257–65.

[10] Grant PA, Duggan L, Cote J, Roberts SM, Brownell JE, Candau R, et al. Yeast Gcn5 functions in two multisubunit complexes to acetylate nucleosomal histones: characterization of an Ada complex and the SAGA (Spt/Ada) complex. Genes Dev 1997;11(13):1640–50.

[11] Martinez E. Multi-protein complexes in eukaryotic gene transcription. Plant Mol Biol 2002;50(6):925–47.

[12] Zhao Y, Lang G, Ito S, Bonnet J, Metzger E, Sawatsubashi S, et al. A TFTC/STAGA module mediates histone H2A and H2B deubiquitination, coactivates nuclear receptors, and counteracts heterochromatin silencing. Mol Cell 2008;29(1):92–101.

[13] Lang G, Bonnet J, Umlauf D, Karmodiya K, Koffler J, Stierle M, et al. The tightly controlled deubiquitination activity of the human SAGA complex differentially modifies distinct gene regulatory elements. Mol Cell Biol 2011;31(18):3734–44.

[14] Daniel JA, Torok MS, Sun ZW, Schieltz D, Allis CD, Yates 3rd JR, et al. Deubiquitination of histone H2B by a yeast acetyltransferase complex regulates transcription. J Biol Chem 2004;279(3):1867–71.

[15] Henry KW, Wyce A, Lo WS, Duggan LJ, Emre NC, Kao CF, et al. Transcriptional activation via sequential histone H2B ubiquitylation and deubiquitylation, mediated by SAGA-associated Ubp8. Genes Dev 2003;17(21):2648–63.

[16] Zhang XY, Varthi M, Sykes SM, Phillips C, Warzecha C, Zhu W, et al. The putative cancer stem cell marker USP22 is a subunit of the human SAGA complex required for activated transcription and cell-cycle progression. Mol Cell 2008;29(1):102–11.

[17] Minsky N, Shema E, Field Y, Schuster M, Segal E, Oren M. Monoubiquitinated H2B is associated with the transcribed region of highly expressed genes in human cells. Nat Cell Biol 2008;10(4):483–8.

[18] Li X, Seidel CW, Szerszen LT, Lange JJ, Workman JL, Abmayr SM. Enzymatic modules of the SAGA chromatin-modifying complex play distinct roles in Drosophila gene expression and development. Genes Dev 2017;31(15):1588–600.

[19] Tang J, Gifford CC, Samarakoon R, Higgins PJ. Deregulation of negative controls on TGF-beta1 signaling in tumor progression. Cancers (Basel) 2018;10(6).

[20] Feng T, Dzieran J, Yuan X, Dropmann A, Maass T, Teufel A, et al. Hepatocyte-specific Smad7 deletion accelerates DEN-induced HCC via activation of STAT3 signaling in mice. Oncogenesis 2017;6(1):e294.

[21] Xia H, Ooi LL, Hui KM. MicroRNA-216a/217-induced epithelial-mesenchymal transition targets PTEN and SMAD7 to promote drug resistance and recurrence of liver cancer. Hepatology 2013;58(2):629–41.

[22] Wang J, Zhao J, Chu ES, Mok MT, Go MY, Man K, et al. Inhibitory role of Smad7 in hepatocarcinogenesis in mice and in vitro. J Pathol 2013;230(4):441–52.

[23] Sun H, Peng Z, Tang H, Xie D, Jia Z, Zhong L, et al. Loss of KLF4 and consequential downregulation of Smad7 exacerbate oncogenic TGF-beta signaling in and promote progression of hepatocellular carcinoma. Oncogene 2017;36(21):2957–68.

[24] Wang C, Sun H, Zou R, Zhou T, Wang S, Sun S, et al. MDC1 functionally identified as an androgen receptor co-activator participates in suppression of prostate cancer. Nucleic Acids Res 2015;43(10):4893–908.

[25] Sun S, Zhong X, Wang C, Sun H, Wang S, Zhou T, et al. BAP18 coactivates androgen receptor action and promotes prostate cancer progression. Nucleic Acids Res 2016;44(17):8112–28.

[26] Tang Z, Li C, Kang B, Gao G, Li C, Zhang Z. GEPIA: a web server for cancer and normal gene expression profiling and interactive analyses. Nucleic Acids Res 2017;45(W1):W98–W102.

[27] Gao WW, Xiao RQ, Zhang WJ, Hu YR, Peng BL, Li WJ, et al. JMJD6 licenses ERalpha-dependent enhancer and coding gene activation by modulating the recruitment of the CARM1/MED12 co-activator complex. Mol Cell 2018;70(2) 340-57 e8.

[28] Lin CY, Strom A, Vega VB, Kong SL, Yeo AL, Thomsen JS, et al. Discovery of estrogen receptor alpha target genes and response elements in breast tumor cells. Genome Biol 2004;5(9):R66.

[29] Tu CC, Kumar VB, Day CH, Kuo WW, Yeh SP, Chen RJ, et al. Estrogen receptor alpha (ESR1) over-expression mediated apoptosis in Hep3B cells by binding with SP1 proteins. J Mol Endocrinol 2013;51(1):203–12.

[30] Shema E, Tirosh I, Aylon Y, Huang J, Ye C, Moskovits N, et al. The histone H2B-specific ubiquitin ligase RNF20/hBRE1 acts as a putative tumor suppressor through selective regulation of gene expression. Genes Dev 2008;22(19):2664–76.

[31] Tarcic O, Granit RZ, Pateras IS, Masury H, Maly B, Zwang Y, et al. RNF20 and histone H2B ubiquitylation exert opposing effects in Basal-Like versus luminal breast cancer. Cell Death Differ 2017;24(4):694–704.

[32] Wang E, Kawaoka S, Yu M, Shi J, Ni T, Yang W, et al. Histone H2B ubiquitin ligase RNF20 is required for MLL-rearranged leukemia. Proc Natl Acad Sci U S A 2013;110(10):3901–6.

[33] Blank M, Tang Y, Yamashita M, Burkett SS, Cheng SY, Zhang YE. A tumor suppressor function of Smurf2 associated with controlling chromatin landscape and genome stability through RNF20. Nat Med 2012;18(2):227–34.

[34] Tang B, Liang X, Tang F, Zhang J, Zeng S, Jin S, et al. Expression of USP22 and Survivin is an indicator of malignant behavior in hepatocellular carcinoma. Int J Oncol 2015;47(6):2208–16.

[35] Zhai R, Tang F, Gong J, Zhang J, Lei B, Li B, et al. The relationship between the expression of USP22, BMI1, and EZH2 in hepatocellular carcinoma and their impacts on prognosis. Onco Targets Ther 2016;9:6987–98.

[36] Ling S, Li J, Shan Q, Dai H, Lu D, Wen X, et al. USP22 mediates the multidrug resistance of hepatocellular carcinoma via the SIRT1/AKT/MRP1 signaling pathway. Mol Oncol 2017;11(6):682–95.

[37] Naugler WE, Sakurai T, Kim S, Maeda S, Kim K, Elsharkawy AM, et al. Gender disparity in liver cancer due to sex differences in MyD88-dependent IL-6 production. Science 2007;317(5834):121–4.

[38] Prieto J. Inflammation, HCC and sex: IL-6 in the centre of the triangle. J Hepatol 2008;48(2):380–1.

[39] Shi L, Feng Y, Lin H, Ma R, Cai X. Role of estrogen in hepatocellular carcinoma: is inflammation the key? J Transl Med 2014;12:93.

[40] Hishida M, Nomoto S, Inokawa Y, Hayashi M, Kanda M, Okamura Y, et al. Estrogen receptor 1 gene as a tumor suppressor gene in hepatocellular carcinoma detected by triple-combination array analysis. Int J Oncol 2013;43(1):88–94.

[41] Wang SH, Yeh SH, Lin WH, Yeh KH, Yuan Q, Xia NS, et al. Estrogen receptor alpha represses transcription of HBV genes via interaction with hepatocyte nuclear factor 4alpha. Gastroenterology 2012;142(4) 989-98 e4.

[42] Liu WH, Yeh SH, Lu CC, Yu SL, Chen HY, Lin CY, et al. MicroRNA-18a prevents estrogen receptor-alpha expression, promoting proliferation of hepatocellular carcinoma cells. Gastroenterology 2009;136(2):683–93.

[43] Wu H, Yao S, Zhang S, Wang JR, Guo PD, Li XM, et al. Elevated expression of Erbin destabilizes ERalpha protein and promotes tumorigenesis in hepatocellular carcinoma. J Hepatol 2017;66(6):1193–204.

[44] Samara NL, Datta AB, Berndsen CE, Zhang X, Yao T, Cohen RE, et al. Structural insights into the assembly and function of the SAGA deubiquitinating module. Science 2010;328(5981):1025–9.

[45] Fuchs G, Hollander D, Voichek Y, Ast G, Oren M. Cotranscriptional histone H2B monoubiquitylation is tightly coupled with RNA polymerase II elongation rate. Genome Res 2014;24(10):1572–83.

[46] Prenzel T, Begus-Nahrmann Y, Kramer F, Hennion M, Hsu C, Gorsler T, et al. Estrogen-dependent gene transcription in human breast cancer cells relies upon proteasome-dependent monoubiquitination of histone H2B. Cancer Res 2011;71(17):5739–53.

[47] Bedi U, Scheel AH, Hennion M, Begus-Nahrmann Y, Ruschoff J, Johnsen SA. SUPT6H controls estrogen receptor activity and cellular differentiation by multiple epigenomic mechanisms. Oncogene 2015;34(4):465–73.

[48] Reid G, Hubner MR, Metivier R, Brand H, Denger S, Manu D, et al. Cyclic, proteasome-mediated turnover of unliganded and liganded ERalpha on responsive promoters is an integral feature of estrogen signaling. Mol Cell 2003;11(3):695–707.

[49] Tateishi Y, Kawabe Y, Chiba T, Murata S, Ichikawa K, Murayama A, et al. Ligand-dependent switching of ubiquitin-proteasome pathways for estrogen receptor. EMBO J 2004;23(24):4813–23.

[50] Nawaz Z, Lonard DM, Dennis AP, Smith CL, O'Malley BW. Proteasome-dependent degradation of the human estrogen receptor. Proc Natl Acad Sci U S A 1999;96(5):1858–62.

[51] Pijnappel WW, Timmers HT. Dubbing SAGA unveils new epigenetic crosstalk. Mol Cell 2008;29(2):152–4.